

# Phenotypic Screening for Small Molecules that Protect $\beta$ -Cells from Glucolipotoxicity

Jonnell C. Small, Aidan Joblin-Mills, Kaycee Carbone, Maria Kost-Alimova, Kumiko Ayukawa, Carol Khodier, Vlado Dancik, Paul A. Clemons, Andrew B. Munkacsi, and Bridget K. Wagner\*



Cite This: *ACS Chem. Biol.* 2022, 17, 1131–1142



Read Online

ACCESS |

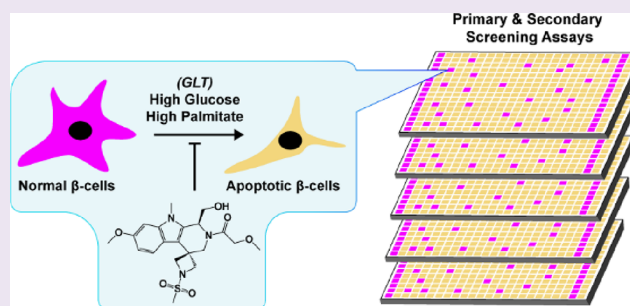
Metrics & More

Article Recommendations

Supporting Information

**ABSTRACT:** Type 2 diabetes is marked by progressive  $\beta$ -cell failure, leading to loss of  $\beta$ -cell mass. Increased levels of circulating glucose and free fatty acids associated with obesity lead to  $\beta$ -cell glucolipotoxicity. There are currently no therapeutic options to address this facet of  $\beta$ -cell loss in obese type 2 diabetes patients. To identify small molecules capable of protecting  $\beta$ -cells, we performed a high-throughput screen of 20,876 compounds in the rat insulinoma cell line INS-1E in the presence of elevated glucose and palmitate. We found 312 glucolipotoxicity-protective small molecules (1.49% hit rate) capable of restoring INS-1E viability, and we focused on 17 with known biological targets. 16 of the 17

compounds were kinase inhibitors with activity against specific families including but not limited to cyclin-dependent kinases (CDK), PI-3 kinase (PI3K), Janus kinase (JAK), and Rho-associated kinase 2 (ROCK2). 7 of the 16 kinase inhibitors were PI3K inhibitors. Validation studies in dissociated human islets identified 10 of the 17 compounds, namely, KD025, ETP-45658, BMS-536924, AT-9283, PF-03814735, torin-2, AZD5438, CP-640186, ETP-46464, and GSK2126458 that reduced glucolipotoxicity-induced  $\beta$ -cell death. These 10 compounds decreased markers of glucolipotoxicity including caspase activation, mitochondrial depolarization, and increased calcium flux. Together, these results provide a path forward toward identifying novel treatments to preserve  $\beta$ -cell viability in the face of glucolipotoxicity.



## INTRODUCTION

Obesity is a critical risk factor for the development of type 2 diabetes (T2D). Elevated levels of free fatty acids (FFA) are observed in obesity because of expanded adipose tissue mass and reduced FFA clearance.<sup>1</sup> Increasing evidence suggests that elevated FFAs may contribute to T2D pathogenesis and represent a mechanistic link between obesity and diabetes. FFAs induce insulin resistance and pancreatic  $\beta$ -cell dysfunction, two major defects underlying T2D pathophysiology.<sup>2</sup> Prolonged FFA exposure has inhibitory effects on insulin secretion.<sup>3</sup> When co-infused with glucose, FFA elevation inhibits the stimulatory effect of hyperglycemia on  $\beta$ -cell function,<sup>3</sup> and individuals genetically predisposed to T2D show increased susceptibility to FFA-dependent  $\beta$ -cell dysfunction.<sup>4,5</sup> Exposure to elevated glucose exerts synergistic effects with FFAs, leading to glucolipotoxicity (GLT).<sup>6–9</sup> GLT is characterized by impaired glucose-stimulated insulin secretion (GSIS), decreased insulin gene transcription, attenuation of  $\beta$ -cell-specific transcription factors PDX1 and MAFA, and induction of apoptosis through activated caspase, mitochondrial depolarization, increased calcium flux, oxidative stress, and the unfolded protein response.<sup>10,11</sup>

The absence of strategies to suppress GLT-induced loss of  $\beta$ -cell function and mass in T2D has inspired the search for  $\beta$ -cell-

protective small molecules. Recent high-throughput screening (HTS) campaigns have identified anti-apoptotic small molecules in  $\beta$ -cell models of lipotoxicity and glucolipotoxicity. These include the polyunsaturated fatty acid amide and endogenous endocannabinoid anandamide,<sup>12</sup> the FDA-approved HER2/EGFR dual kinase inhibitor neratinib,<sup>13</sup> and L-type calcium channel blockers nifedipine and verapamil.<sup>14</sup> Polyunsaturated fatty acids, especially anandamide, protect against saturated fatty acid-induced lipotoxicity by binding to  $\beta$ -cell fatty acid receptors and decreasing uptake of toxic saturated fatty acids. Neratinib is  $\beta$ -cell protective by inhibiting the serine–threonine kinase STK4/MST1, a key regulator of  $\beta$ -cell apoptosis and dysfunction in diabetes. L-type calcium channel blockers like nifedipine and verapamil protect against GLT by decreasing calcium influx, which induces apoptosis. The discovery of these small molecules and their diverse mechanisms of action suggest

Received: January 18, 2022

Accepted: March 14, 2022

Published: April 19, 2022



there are multiple avenues through which  $\beta$ -cell function and survival can be promoted and maintained.

HTS has long been utilized in the pharmaceutical industry for therapeutic discovery, and its application in the academic setting has spurred the discovery of novel biological probes for perturbing and investigating cellular mechanisms.<sup>15</sup> Phenotypic HTS has become especially attractive because such screens preserve the functional cellular context of targets of compounds. Additionally, it allows target-agnostic compound discovery (*i.e.*, identify compounds that induce similar phenotypic changes through different cellular targets). Phenotypic HTS has therefore been very useful in identifying compounds important for  $\beta$ -cell survival, insulin degradation, and  $\beta$ -cell replication.<sup>16–18</sup>

Identifying novel  $\beta$ -cell protective small molecules using phenotypic HTS is advantageous on two fronts. First, it enables the potential discovery of novel mechanisms regulating  $\beta$ -cell survival and function, which can be further investigated to generate a more holistic understanding of  $\beta$ -cell biology. Second, it provides novel chemical matter that can be further optimized to generate lead candidates for the treatment of T2D. Motivated by both questions, we performed a screen of 20,876 compounds in INS-1E cells, with the goal of identifying novel compounds with  $\beta$ -cell protective activity. We identified two diversity-oriented synthesis (DOS)-derived scaffolds with GLT-suppressive activity. We also found 17 small molecules with known biological targets capable of suppressing GLT in both INS-1E cells and human islets. Several of these compounds reveal a critical role for kinase inhibition in promoting  $\beta$ -cell survival and function. These results suggest new mechanisms for promoting  $\beta$ -cell survival and provide further evidence that multiple cellular processes govern the  $\beta$ -cell function in obese and T2D patients.

## RESULTS AND DISCUSSION

**Primary Screen Identifies  $\beta$ -Cell-Protective Compounds.** We performed a primary screen (Figure S1a) in INS-1E cells to identify compounds that protected  $\beta$ -cells from GLT as measured by cell viability detected using CellTiter-Glo. Optimized GLT media contained 25 mM glucose and 0.5 mM sodium palmitate, which induced  $\sim$ 70% INS-1E cell death after 48-h treatment (Figure 1a). Sodium palmitate was the major contributor to INS-1E cell death in GLT conditions *via* reduced INS-1E viability by 25 and 50% at 0.25 and 0.5 mM, respectively, compared to the control (Figure S1d–e). Sodium palmitate is well documented to induce lipotoxicity and glucolipotoxicity in  $\beta$ -cell models including INS-1E, INS-1, BRIN-BD11, and MIN6.<sup>12,19–21</sup>

**Compounds Known to Protect  $\beta$ -Cells Validate Primary Screen Performance.** We selected four chemical libraries (20,876 total compounds) for screening. First, the DOS Informer Set is a subset of the Broad Institute DOS library,<sup>22,23</sup> containing 9510 compounds (192 hits—2.02% hit rate) representing  $\sim$ 30 diverse structural families. Second, the DOS-A library (3840 compounds, 29 hits—0.76% hit rate) is a collection of DOS compounds selected for performance diversity based on a combination of gene expression analysis and cell painting.<sup>24</sup> Finally, the Broad Repurposing Collection (5440 compounds, 81 hits—1.49% hit rate)<sup>25</sup> and Bioactive Libraries (2,086 compounds, 10 hits—0.48% hit rate) contain FDA-approved drugs, candidates in development, and known tool compounds. We screened compounds at a typical screening concentration of 10  $\mu$ M in a 384-well plate format for 48 h to identify those that improved INS-1E viability, as determined by

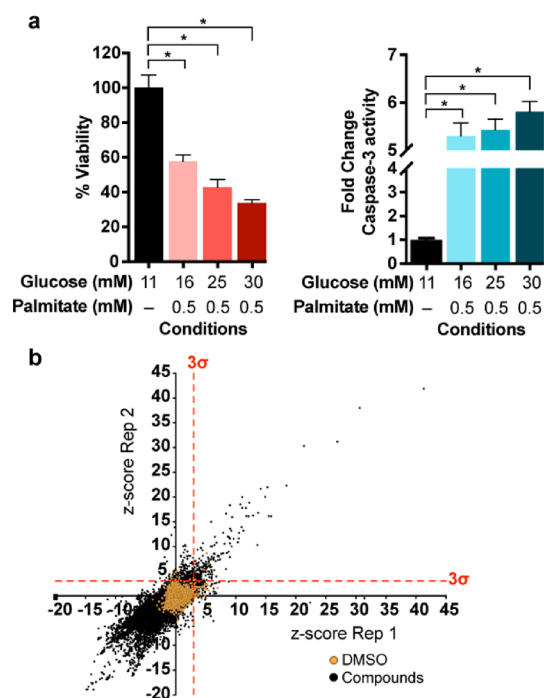


**Figure 1.** Optimization of glucolipotoxicity media for INS-1E cells and phenotypic screening of glucolipotoxicity-suppressing compounds. (a) Cell death and caspase-3 activation are significantly enhanced in GLT media conditions with increasing levels of glucose and 0.5 mM sodium palmitate. \*  $P < 0.0001$ , as determined by unpaired  $t$ -test. (b) Scatter plot showing HTS results from 20,876 compounds (black dots) where compounds were screened at concentrations between 5 and 10  $\mu$ M in duplicate and z-scores were calculated from CellTiter-Glo readouts for compounds relative to the DMSO control using Genedata Screener. A z-score of  $\geq 3$  ( $3\sigma$ ) was used as a threshold for hit calling (red-dotted line).

calculated z-scores (Figure 1b and Table S1). Using a hit-calling threshold of z-score  $\geq 3$  ( $3\sigma$ , relative to DMSO) in two replicates, we identified 312 total hits (1.49% overall hit rate). This hit rate of 1.49% was more than 100 times the average hit rate of 0.01–0.14% for most high-throughput screens.<sup>26</sup> Because of availability, 160 hits were selected for retesting at four concentration points (1.25, 2.5, 5, and 10  $\mu$ M) to determine their effects on INS-1E cell viability and caspase activation in GLT conditions.

Anandamide (AEA), a polyunsaturated fatty acid amide with z-scores  $>40$  in both replicates of the primary screen, was validated as a potent hit with a dose-dependent increase in INS-1E viability and dose-dependent decrease in caspase activity in GLT conditions. AEA recovered  $\sim$ 90 and  $\sim$ 70% of INS-1E viability and decreased caspase activity compared to the basal media control, respectively (Figure 2a). The AEA derivative AM404 (z-scores  $>18$  in both replicates) also showed a similar activity at 10  $\mu$ M, recovering INS-1E viability to  $\sim$ 90% of the control and decreasing caspase activity to 86% of the control (Figure 2b). Our results are consistent with previous studies that confirmed AEA and AM404 as GLT- and lipotoxicity-protective small molecules in INS-1, INS-1E, and BRIN-BD11 cells.<sup>12,20</sup> The monounsaturated fatty acid amide oleoylethanolamide (OEA) exhibited z-scores of  $>6$  in both replicates of the primary screen and showed maximum activity at 10  $\mu$ M where it recovered INS-1E viability to  $\sim$ 60% of control and decreased caspase activity to 33% of control (Figure 2c). Consistently, OEA had also been previously identified as lipotoxicity-

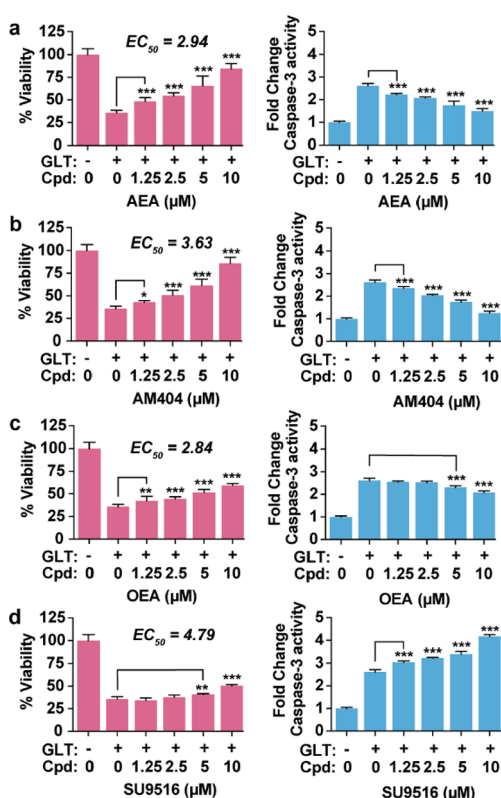


**Figure 2.** Confirmation of GLT-protective activity. Four compounds previously reported to protect against GLT provide proof-of-principle results for the detection of novel bioactivity in the HTS. (a,b) Anandamide (AEA) and the AEA derivative (AM404) increased INS-1E viability and decreased caspase-3 activity in a dose-dependent manner. (c) Oleylethanolamide (OEA) increased INS-1E viability and moderately decreased caspase-3 activity. (d) SU9516 moderately protected at 5 and 10  $\mu\text{M}$ , with more dramatically increased caspase-3 activation. Data represent mean  $\pm$  SD of 5 replicates. Statistical significance was evaluated using an unpaired, one-tailed *t*-test for each compound compared to GLT alone (\*  $P < 0.05$ ; \*\*  $P < 0.001$ ; \*\*\*  $P < 0.0001$ ).

protective in BRIN-BD11 cells.<sup>20</sup> SU9516 (*z*-scores  $> 9$  in both replicates) recovered only 65% of its INS-1E viability compared to control, and this was associated with an increase in caspase activity using the Caspase-Glo 3/7 assay (Figure 2d). Similar to the aforementioned compounds, SU9516 has been shown to be GLT-protective in INS-1 cells.<sup>12</sup> Literature confirmation of primary screen hits AEA, AM404, OEA, and SU9516 provided evidence that the primary screen successfully identified GLT-protective small molecules from the four libraries.

Through initial validation studies confirming primary screen hits AEA, AM404, OEA, and SU9516 utilized the CellTiter-Glo reagent, we learned that this reagent can yield false-positive results. Apitolisib showed a dose-dependent increase in luminescence with the CellTiter-Glo readout, suggesting that it was a GLT-protective compound; however, this activity was not validated with cell number quantification using nuclear staining (Figure S2a,b). High-content microscopy revealed that apitolisib did not proportionally increase the INS-1E cell number above that of control cells treated with GLT and DMSO. We speculated that apitolisib induced changes in cellular ATP levels in INS-1E that resulted in increased CellTiter-Glo luminescence. We, therefore, developed a high-content fluorescent microscopy (HCFM) assay utilizing the

live-cell-impermeable dye DRAQ7<sup>27–29</sup> and the CellEvent Caspase-3/7 dye<sup>30,31</sup> to quantify total number of live (DRAQ7-negative, caspase-negative) cells and percent viability (% DRAQ7 negative, caspase negative cells) (Figure S2b,c). This assay revealed that while some compounds were able to increase percent viability, they had little or no effect on the total number of live cells (as was the case for apitolisib). The decrease in caspase-3 activation by apitolisib detected *via* Caspase Glo and the HCFM assay was not associated with an increase in cell number, and we speculate that apitolisib may be arresting INS-1E cell growth while protecting the viability of the non-mitotic cells. The HCFM assay is therefore appropriate for high-throughput investigations of cell viability, especially in GLT where it generated *Z'*-factor values  $> 0.4$  (Figure S2d,e). The HCFM assay was subsequently used in validation studies of primary screen hits.

**Azetidone Monoketopiperazine and Pictet-Spengler Scaffolds Protect INS-1E Cells from GLT.** Many of the DOS primary hits came from the azetidone monoketopiperazine<sup>32</sup> (AMK, 1.25% hit-rate) and Pictet–Spengler<sup>33</sup> (0.63% hit-rate) libraries (Figure 3a–c). We observed structure–activity relationships (SAR) that defined active and inactive compounds (Figure 3d,e, Tables 1, and 2). For AMK compounds, stereochemistry around the monoketopiperazine core was a key determinant of activity (Figure 3c). BRD4935 (*R,S,S* stereochemistry in the monoketopiperazine core) was the most potent AMK compound, recovering INS-1E viability to 100% of AEA control (Figure 3d). Stereochemistry around the monoketopiperazine core became less of a predictor of activity among AMK compounds containing different *R*<sub>1</sub> and *R*<sub>2</sub> groups. BRD3476 (*S,R,S*) was the second most active AMK compound and at 2.96  $\mu\text{M}$  increased the number of live INS-1E cells nearly threefold over that of the GLT control, while recovering INS-1E viability to 70% (Figure 3d).

In general, Pictet–Spengler (PS) library members were more active than AMK members. BRD4189 (**1**), the most potent PS hit, recovered a maximum of 51% of INS-1E viability compared with the basal media control using the CellTiter-Glo reagent and about 100% of the AEA control using the HCFM assay (Table 1, Figure 3e). The identity of the *R*<sub>1</sub> and *R*<sub>2</sub> side chains of the azetidone (magenta) and piperidine (gold) spirocyclic tetrahydroharmane (THH) cores drastically affected PS compound activity. For example, with the same *S* stereochemistry, **1** was 20% more active than **5** but only 3% more active than **6** (BRD2892) (Table 1). However, stereochemistry of the methylhydroxyl group on the spirocyclic azetidone-THH cores had a significant effect on activity. While **1** (*S* stereochemistry) recovered 51.3% of INS-1E viability compared to the basal media control and 100% compared to the AEA control, BRD6618 (**2**) (*R* stereochemistry) recovered 12.6% of INS-1E viability compared to the basal media control and 50% compared to the AEA control (Table 1 and Figure 3E). For spirocyclic piperidine–THH compounds, changing the stereochemistry of the methylhydroxyl group moderately affected activity. **8** (*S* stereochemistry) recovered 48% of its INS-1E viability compared to the control, while **9** (*R* stereochemistry) recovered 42.9% of its INS-1E viability (Table 2). One exception is made for compound **20**, which when inverted to *S* stereochemistry (**21**) lost more than 25% activity (Table 2). The azetidone–THH scaffold BRD4189 (**1**) was the most GLT-protective small molecule of the DOS compounds tested and provides a promising novel compound class for future structure–activity relationship and mechanism-of-action inves-

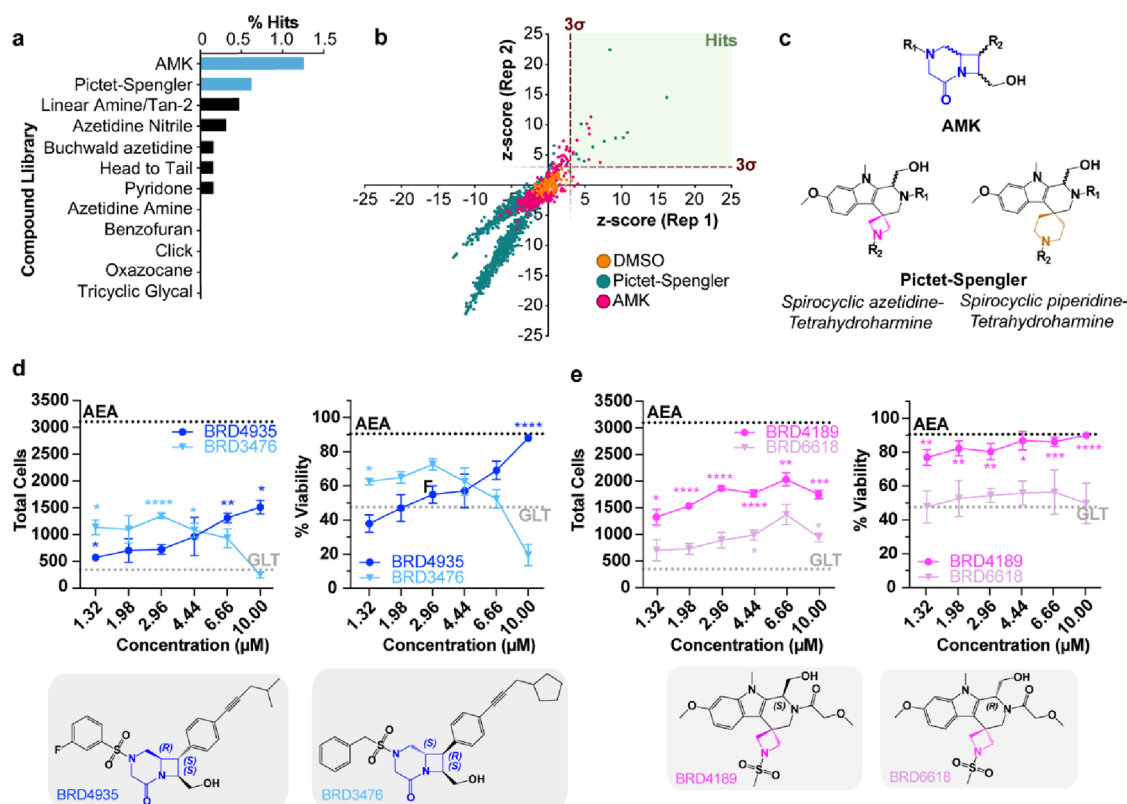


**Figure 3.** Validation of GLT-protective compounds in the Pictet-Spengler and Azetidine monoketopiperazine (AMK) libraries. (a) Hit-rate distribution across compound libraries within the DOS Informer Set. Light blue bars indicate the AMK and Pictet-Spengler libraries from which hit compounds BRD4935 and BRD4189 were found. (b) Scatter plot showing results of the Pictet-Spengler and AMK libraries (1920 compounds); compounds were screened at 10  $\mu\text{M}$ . A z-score of 3 ( $3\sigma$ ) was used as a threshold for hit calling (red-dotted line). Data points in yellow, teal, and pink represent the DMSO control, the Pictet-Spengler library, and the AMK library, respectively. (c) Compounds in the AMK library contain a monoketopiperazine core (blue) with three chiral carbons (wavy bonds) and two R groups ( $R_1$  and  $R_2$ ). Compounds in the Pictet-Spengler library contains two spirocyclic  $\beta$ -carboline cores with either an azetidone (magenta) or piperidine (gold) ring, in addition to two R groups ( $R_1$  and  $R_2$ ) and one chiral carbon (wavy bond). (d,e) Dose-dependent increases in GLT protection were validated in INS-1E cells for BRD4935 ( $n = 3$ , from the AMK library), BRD3476 ( $n = 3$ , from the AMK library), and BRD4189 ( $n = 3$ , from the Pictet-Spengler library) using the HCFM assay where INS-1E cells were treated with GLT media and compounds for 48 h. The decreased potency BRD6618 highlights the crucial role of stereochemistry in the activity of BRD4189. Statistical significance was evaluated using an unpaired, one-tailed  $t$ -test for each compound compared to GLT alone (\*  $P < 0.05$ ; \*\*  $P < 0.01$ ; \*\*\*  $P < 0.001$ ; \*\*\*\*  $P < 0.0001$ ).

tigations. To rule out promiscuity, we also performed cross-reactivity analysis<sup>34</sup> on BRD4189 and several other spirocyclic azetidone-THH compounds. We found that these compounds were not frequent hits in other screening assays (Table S4).

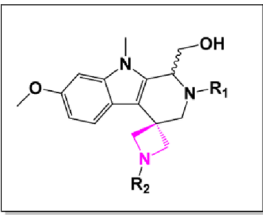
**Acetyl-CoA Carboxylase Inhibition Protects  $\beta$ -Cells From GLT.** CP-640186 is identified as a novel  $\beta$ -cell GLT-protective small molecule with nanomolar potency. We validated CP-640186 as a potent GLT-protective small molecule that recovered 97% of INS-1E viability compared to the control with an  $\text{EC}_{50}$  of 410 nM (Figure S3, Table S2). CP-640186 is an isozyme-nonspecific acetyl-CoA carboxylase (ACC) inhibitor that inhibits fatty acid synthesis, fatty acid oxidation, and triglyceride synthesis.<sup>35</sup> The identification of CP-640186 as GLT protective was an intriguing result in our study. This result was further validated in INS-1E cells *via* reductions in GLT-induced mitochondrial depolarization and calcium influx (Figures 4a, 5g). While we are not sure these are specific mechanisms of CP-640186 GLT-protectivity, ample literature evidence indicates that decreasing calcium influx improves  $\beta$ -cell function and viability.<sup>14</sup> CP-640186 was first identified for its ability to reduce fatty acid synthesis and increase fatty acid oxidation.<sup>35</sup> In the context of  $\beta$ -cell GLT, these activities likely decrease the fatty load in  $\beta$ -cells and allow them to circumvent

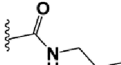
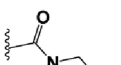
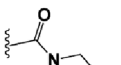
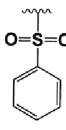
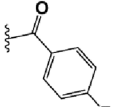
the deleterious effects associated with fatty acid accumulation. There are currently no FDA-approved ACC inhibitors; however, given the crucial role fatty acid metabolism plays in cell viability, ACC inhibition is being explored as a potential therapeutic strategy in several diseases including nonalcoholic fatty liver disease (NAFLD) and non-alcoholic steatohepatitis (NASH). ACC inhibition is therefore a potentially beneficial therapeutic strategy for the treatment of T2D.

#### Numerous Kinase Inhibitors Protect $\beta$ -Cells From GLT.

Several lead compounds from the Broad Repurposing Collection were annotated kinase inhibitors (Table S2). We found that 623 of the 4829 compounds with annotated targets had at least one kinase as a target, and that of these, 58 were screening hits (nominal  $p$ -value  $1.8 \times 10^{-22}$ ). These included inhibitors of cyclin-dependent kinases (CDK) [AZD5438 and palbociclib], PI-3 kinase (PI3K) [AZD8186, TGX-221, PIK-93, ETP-45658, taselisib (GDC-0032), GSK2126458 (omipalisib), and duvelisib], mTOR (ETP-46464 and torin-2), Rho-associated kinase 2 (ROCK2) [KD025 (SLX-2119)], JAK2 (LY2784544 and AT-9283), and Aurora A/B kinase (PF-03814735). Using the HCFM assay, we calculated  $\text{EC}_{50}$  values for these kinase inhibitors and identified ETP-45658, ETP-46464, PIK-93, taselisib, and GSK2126458 as potent com-

**Table 1. Maximum Recovered Viability and EC<sub>50</sub> (μM) Values of Structurally Related Spirocyclic Azetidine-β-Carbolines in the DOS Library**

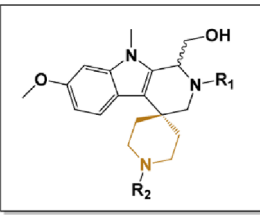


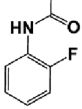
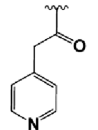
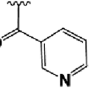
	R <sub>1</sub>	R <sub>2</sub>	Stereochemistry	z-score <sub>1</sub>	z-score <sub>2</sub>	Max Recovered Viability (%)	EC <sub>50</sub> (μM)
1			S	4.52	7.28	51.3	1.79
2		"	R	1.10	1.33	12.6	3.38
3		"	S	3.56	2.98	39.2	4.18
4		"	R	-1.43	-1.77	9.0	4.82
5			S	3.73	4.61	29.5	4.35
6			S	3.07	4.07	48.2	2.19
7			S	3.71	2.89	26.1	3.24

pounds that recovered > 85% of INS-1E viability compared to control (Figure S3, Table S2). The kinase inhibitor neratinib was previously identified as GLT-protective in INS-1E and rodent models.<sup>13</sup> The mechanism by which it was shown to be GLT-protective was *via* STK4/MST1 inhibition, a novel activity for the FDA-approved dual HER2/EGFR inhibitor. Our study reveals that a wide selection of inhibitors against several kinase families are β-cell-protective, suggesting a variety of kinases regulate beta-cell viability and function. However, further studies will be needed to investigate whether these kinases are their β-cell relevant targets, or if, like neratinib, other novel targets are responsible. We also found that several of these kinases were able to partially restore Pdx1 expression in INS-1E cells treated with GLT media (Figure S4). Pdx1 is a β-cell-specific transcription factor and its expression is known to decrease in β-cells experiencing GLT.<sup>13,36</sup> Encouragingly, top hits ETP-45658, ETP-46464, PIK-93, and tasiselisib significantly restored Pdx1 expression.

**Decreased Calcium Flux and Mitochondrial Re-Polarization Coincide with GLT-Protectivity.** The significance of calcium flux and calcium signaling in β-cell survival and health has recently been implicated *via* the identification of compounds that protected INS-1E cells from GLT by decreasing cellular calcium content.<sup>14</sup> GLT treatment impairs β-cell calcium flux

and specifically increases β-cell calcium content. Using the Calcium 6 dye that generates a fluorescent signal upon binding to intracellular calcium, we tested whether the kinase inhibitors decreased cellular calcium influx in INS-1E cells treated with GLT media.<sup>37</sup> KD025 significantly decreased calcium influx to levels below that of the GLT control at all concentrations tested (2.5–10 μM) (Figure 4a). ETP-45658, ETP-46464, PIK-93, tasiselisib, duvelisib, palbociclib, TGX-221, and AZD8186 moderately decreased calcium flux to levels below that of the GLT control (2.5–10 μM) (Figure 4a). Additionally, we found that the ACC1 inhibitor CP-640186, a non-kinase inhibitor, significantly decreased GLT-induced calcium influx (Figure 4a). All other six compounds (torin-2, GSK2126458, LY2784544, AT-9283, BMS-536924, and PF-03814735) either had no effect on calcium influx or increased calcium influx (Figure 4b). Because not all Repurposing Library hits decreased cellular calcium flux, we conclude that β-cell protection from GLT can be achieved without lowering cellular calcium content. GLT is also known to affect mitochondrial function; therefore, we investigated mitochondrial polarity using flow cytometry and the JC-1 dye.<sup>2,38</sup> Mitochondria were depolarized in INS-1E cells treated with GLT media for 48 h (Figure 5a–g). Several of our lead compounds (ETP-45658, ETP-46464, PIK-93, KD025, and CP-640186) reduced GLT-induced mitochondrial depolariza-

Table 2. Maximum Recovered Viability and EC<sub>50</sub> (μM) Values of Structurally Related Spirocyclic Piperidine-β-Carbolines in the DOS Library


	R <sub>1</sub>	R <sub>2</sub>	Stereochemistry	z-score <sub>1</sub>	z-score <sub>2</sub>	Max Recovered Viability (%)	EC <sub>50</sub> (μM)
8			S	6.50	5.87	48.0	1.55
9		"	R	2.89	3.18	42.9	1.80
10		"	R	3.04	3.99	50.4	1.69
-----							
11			R	2.83	6.00	30.4	2.99
12		"	S	1.68	3.69	48.3	4.05
13		"	R	3.39	2.48	45.5	1.80
14		"	S	2.36	2.92	35.3	3.87
15		"	R	2.84	1.34	N/A	N/A
-----							
16			R	1.17	3.03	29.1	5.27
20		"	R	1.90	4.43	30.6	4.96
21		"	S	3.42	1.57	9.7	3.67
-----							
22			R	2.57	3.20	18.2	5.20
23			S	1.49	2.79	38.0	4.99

tion (Figure 5c–g). The most potent reduction of mitochondrial depolarization was observed with ETP-45658 and CP-640186 (Figure 5c,g).

**GLT-Protective Compounds Can Decrease Cytokine Mediated β-Cell Death.** We next sought to determine the specificity of GLT-protective compounds by measuring their effects on proinflammatory cytokine-induced stress. We treated INS-1E cells with a cocktail of IL-1β, IFN-γ, and TNF-α without GLT for 48 h and quantified viability using the HCFM assay. Several compounds (AT-9283, LY2784544, AZD5438, PF-03814735, and BMS-536924) significantly recovered INS-1E viability in the presence of cytokines (Figure S6). AT-9283 and

LY2784544 are both JAK inhibitors and JAK inhibition is known to protect diabetic mice and β-cells from cytokine-mediated stress.<sup>39,40</sup> AZD5438 is a CDK 1,2, and 9 inhibitor. PF-03814735 and BMS-536924 are multitarget kinase inhibitors with nanomolar potency against several kinase families. The compounds AZD8186, duvelisib, ETP-45658, ETP-46464, KD025, palbociclib, and PIK-93 were toxic at concentrations above 1 μM. GSK2126458, taselib, and torin-2 were toxic at all concentrations tested with cytokine treatment. CP-640186 and TGX-221, though nontoxic, did not recover INS-1E viability. These results indicate that less than half of the 17 GLT-protective hits were generally β-cell-protective.

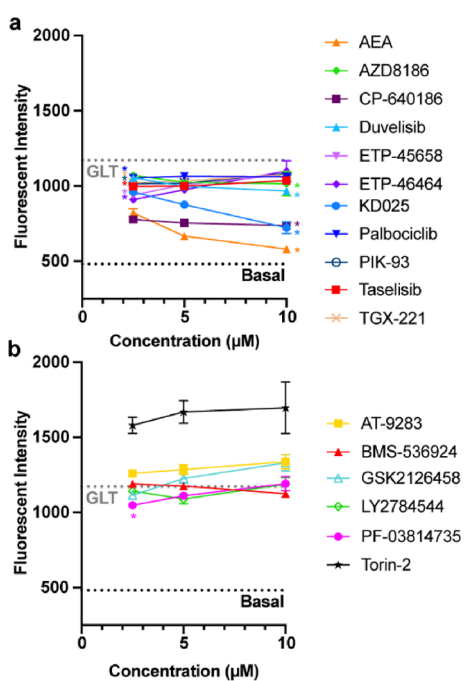


**Figure 4.** Lead compounds protect against GLT *via* decreased calcium flux. (a,b) INS-1E cells incubated with Calcium 6 dye to detect cellular calcium content ( $n = 3$ ). Relative to GLT treatment that increased fluorescent intensity in INS-1E cells (*i.e.*, compare fluorescent intensity for the basal media control and the GLT control), there were (a) compounds that significantly decreased GLT-induced calcium flux in a dose-dependent manner as well as (b) compounds that had little effect on decreasing GLT induced calcium flux. All compounds were treated at  $n = 3$ . The black dotted line ( $n = 72$ ) represents the fluorescent intensity of INS-1E cells incubated in basal culture media. The gray dotted line ( $n = 32$ ) represents the fluorescent intensity of INS-1E cells treated with GLT media and DMSO. Statistical significance was evaluated using an unpaired, one-tailed *t*-test for each compound compared to GLT alone ( $* P < 0.0001$ ).

**Validation in Human Islets.** To further validate the Repurposing Library hits, we tested these compounds in human islets and pancreatic cells that include  $\beta$ -cells and exhibit reduced function in obesity and T2D. Induction of GLT decreased the percent of C-peptide-positive cells by 25% in dissociated islet cells acquired from three donors (Figure 6). C-peptide is produced in the maturation of insulin. Preproinsulin, translated from insulin mRNA, is cleaved into mature insulin in the ER *via* the excision of a signal peptide and its C-peptide domains.<sup>41</sup> Therefore, there is a stoichiometric equivalence of C-peptide and mature insulin within  $\beta$ -cells, and C-peptide can be used as an alternative insulin detection/quantification method. C-peptide staining is often used to quantify beta-cell abundance in patient islets or to quantify blood insulin levels.<sup>42</sup> T2D islets are known to show decreased staining for C-peptide, indicating decreased  $\beta$ -cell mass in these patients. In a potentially therapeutic manner, several compounds (KD025, AZD5438, PF-03814735, ETP-45658, CP-640186, torin-2, BMS-536924, ETP-46464, GSK2126458, AT-9283, and AT-9283) significantly increased percent C-peptide-positive cells (Figure 6). KD025 increased percent C-peptide-positive cells to 110% of basal media (*i.e.*, no evidence of GLT) in several donor samples. Likewise, the other lead compounds (AZD5438, PF-03814735, ETP-45658, CP-640186, torin-2, BMS-536924, and ETP-46464) increased percent C-peptide-positive cells, albeit these improvements varied between 85–90% compared to the

control. CP-640186 was mildly beneficial in human islets increasing the percentage of C-peptide positive cells to approximately 85% that of the control. The remaining compounds were found to be either inactive or toxic (Figure 6). Overall, these results in islets validate our results in  $\beta$ -cells and demonstrate these compounds are consistent with the therapeutic strategy of treating diabetes by decreasing  $\beta$ -cell loss in patients.

## CONCLUSIONS

In summary, the results of our HTS screen in INS-1E cells and subsequent validation in islets provide new tool compounds for the investigation of  $\beta$ -cell biology in the context of T2D and GLT. Several secondary screening approaches enabled us to eliminate toxic compounds and false positives, which ultimately led to the identification of the herein described  $\beta$ -cell-protective small molecules. Previously validated compounds AEA, AM404, OEA, and SU9516 were identified as GLT protective in our primary screen, in addition to two DOS-derived chemical scaffolds, an ACC inhibitor, and 16 kinase inhibitors. It was notable that we identified seven phosphoinositide 3-kinase (PI3K) inhibitors to be protective against GLT (Table S2). The PI3K/Akt/FoxO1 signaling pathway has long been implicated in the protection of  $\beta$ -cells from lipotoxic and glucolipotoxic stress.<sup>43,44</sup> Our findings contrast with this view and suggest that PI3K signaling may be dispensable for  $\beta$ -cell survival. There are four isoforms of PI3K ( $\alpha$ ,  $\beta$ ,  $\delta$ , and  $\gamma$ ) and partial inhibition of one over the other can have different cellular effects. PI3K $\beta$  inhibition, for example, is known to induce the differentiation and maturation of human embryonic stem cells to  $\beta$ -cells and increase insulin expression.<sup>45</sup> ETP-45658, PIK-93, tasislib, GSK2126458, duvelisib, and AZD8186 all share potent activity toward PI3K $\delta$ . It is thus possible that these annotated PI3K inhibitors are protective against GLT *via* specific PI3K isoforms and their cellular targets. Future studies examining kinase profiling and gene expression will help shed light on this uncertainty as well as reveal new mechanisms integral to the complex biology underlying the health and survival of  $\beta$ -cells in obesity and T2D.

## METHODS

**Cell Culture.** INS-1E cells (generously provided by Claes Wollheim and Pierre Maechler, the University of Geneva, Switzerland) were cultured in RPMI 1640 supplemented with 10% FBS, 1% Pen/Strep, 1% sodium pyruvate, and 50  $\mu$ M  $\beta$ -mercaptoethanol. Cells were maintained in flasks precoated with diluted supernatant (1:10) from the rat 804G cell line (804G matrix). 804G cells are a rat cancer cell line known to secrete a laminin-5 rich extracellular matrix. 804G cells were a generous gift from the Susan Bonner-Weir Lab, Joslin Diabetes Center. The 804G matrix induces spreading, improves glucose-stimulated insulin secretion, and increases the survival and proliferation of rat pancreatic  $\beta$ -cells.<sup>46</sup> GLT media for INS-1E consisted of RPMI 1640 supplemented with 1% FBS, 1% Pen/Strep, 1% fatty acid-free BSA, 50  $\mu$ M  $\beta$ -mercaptoethanol, 25 mM glucose, and 0.5 mM sodium palmitate. Sodium palmitate was dissolved in warmed 4% BSA in PBS before being added to RPMI1650.

**Human Islets.** Islets were obtained from the Integrated Islet Distribution Program (IIDP) and Prodo Laboratories, and cultured in CMRL 1066 supplemented with 10% FBS, 1% Pen/Strep, and 2 mM GlutaMAX. Islets were washed with PBS, incubated with accutase for 20 min at 37  $^{\circ}$ C, and cell culture media added to terminate enzymatic dissociation. Cells were then strained, counted, and plated on flasks pretreated with conditioned media from the human bladder carcinoma cell line HTB-9.<sup>47</sup> GLT media for human islets consisted of CMRL

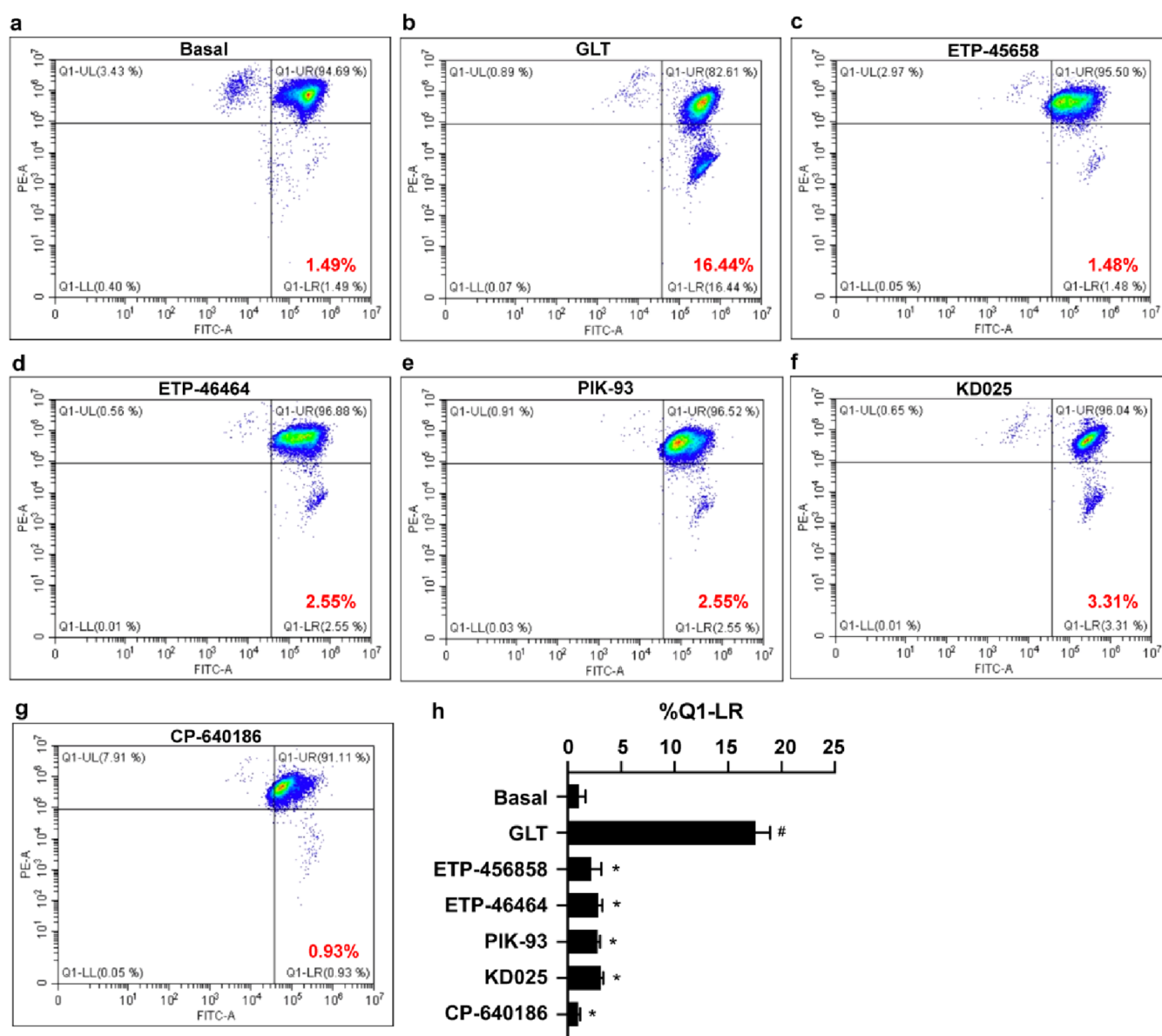


**Figure 5.** Lead compounds protect against GLT *via* decreased mitochondrial depolarization. (a–g) INS-1E cells incubated with JC-1 dye to detect mitochondrial depolarization ( $n = 3$ ). For more gating details, see Figure S5. (a) JC-1 accumulates in polarized mitochondria and emits red/green fluorescence at a 1:1 ratio. (b) Moderate mitochondrial depolarization in INS-1E cells as indicated by the decrease in the red/green ratio. (c,d) ETP-45658, ETP-46464, PIK-93, KD025, and CP-640186 improve GLT-induced mitochondrial depolarization. Representative flow graphs from three experiments. (h) Quantification of flow cytometry detection of mitochondrial depolarization ( $n = 3$ ). Statistical significance was evaluated using an unpaired, one-tailed  $t$ -test (#  $P < 0.001$ —Basal *vs* GLT; \*  $P < 0.0001$  GLT *vs* compound).

1066 supplemented with 1% fatty acid-free BSA, 1% FBS, 30 mM glucose, and 1 mM sodium palmitate.

**High-Throughput Screening.** INS-1E cells were plated at 5000 cells/well in 384-well plates pretreated with supernatant from 804G cells. After 24 h in regular media conditions, media was removed from plates using a Multidrop Combi plate dispenser (ThermoFisher), and GLT media was added at 35  $\mu$ L/well. Following 48 h incubation in GLT media, plates were left to equilibrate to room temperature before CellTiter-Glo (Promega) was added. Luminescence (viability) was quantified using an Envision plate reader (PerkinElmer). A  $3\text{-}\sigma$  ( $z$ -score  $\geq 3$ ) cut-off was used to identify hit compounds from the primary screen, which were then retested at four concentrations. CaspaseGlo (Promega) was also used to quantify caspase-3/7 activity.

**Z' and Z-Score Calculations.** The Z' factor was calculated as previously described using Genedata Screening software (Genedata).<sup>48</sup> The Z-score was calculated using Genedata Screener software (Genedata).

**Compounds.** Compounds in the DOS Informer, DOS-A, Repurposing, and Bioactive libraries were maintained in the Broad Institute and printed into 96- and 384-well plates using a Tecan D300e drug printer. A subset of the repurposed compounds was purchased commercially for validation studies: PIK-93, GSK2126458 (Omipalisib), Duvelisib (IPI-145, INK1197), KD025 (SLx-2119), LY2784544, Palbociclib, Torin-2, AZD8186, AT-9283, and AZD5438 (Selleckchem); ETP-45658 (R&D Systems); ETP-46464, CP-640186, and BMS-536924 (Sigma-Aldrich); PF-03814735, TGX-221, and Taselisib (GDC-0032) (Cayman Chemical); anandamide (VWR Scientific); AM404 (Santa Cruz Biotech) and oleylethanolamide (Combi Blocks). Stock solutions were prepared in DMSO and stored as per manufacturer's instructions.

**Target Enrichment.** To evaluate the screening results from the repurposing collection, we imported target annotation from the Broad Repurposing Hub (clue.io/repurposing-app) and filtered for compounds with annotating targets (4829 of the 5440 screened). We then

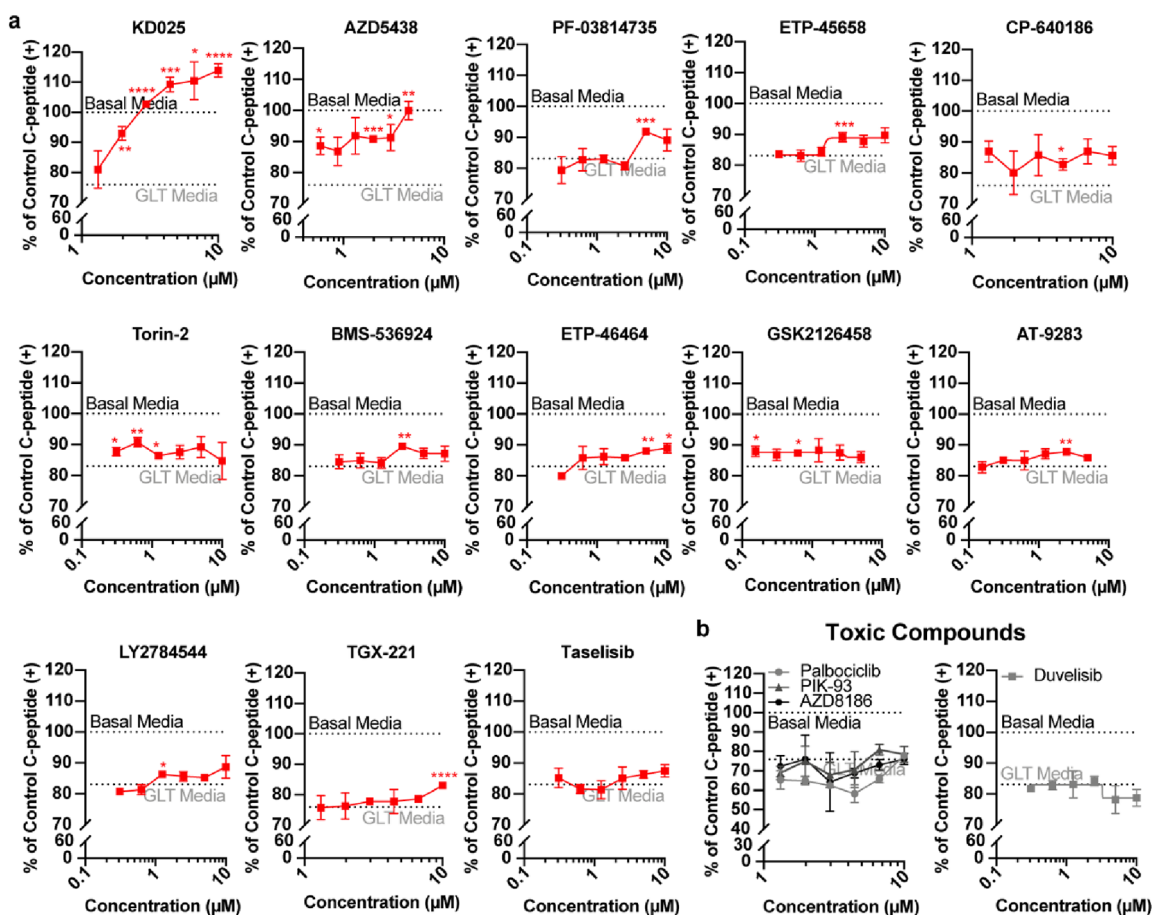


**Figure 6.** Compounds protective against GLT in INS-1E cells are also protective in human islets. Quantification of percent C-peptide positive cells relative to the basal media control revealed (a) compounds active in INS-1E cells and human islets and (b) compounds active in INS-1E cells but inactive or toxic in human islets ( $n = 3$  for all compounds). The black dotted line ( $n = 10$  or  $18$ ) represents the normalized percent of C-peptide positive cells in dissociated human islets incubated in basal culture media for 48 h. The gray dotted line ( $n = 10$  or  $18$ ) represents the normalized percent of C-peptide positive cells in dissociated human islets incubated in GLT media for 48 h. These results are representative data from 1–3 donors (Table S3). Statistical significance was evaluated using an unpaired, one-tailed  $t$ -test for each compound compared to GLT alone (\*  $P < 0.05$ ; \*\*  $P < 0.005$ ; \*\*\*  $P < 0.0005$ ; \*\*\*\*,  $P < 0.00005$ ).

imported a list of gene symbols for 401 human kinases from DiscoverX KinomeScan (<https://www.discoverx.com/services/drug-discovery-development-services/kinase-profiling/kinomescan/gene-symbol>) and found that 623 of the 4829 compounds had at least one kinase inhibitory activity. Of the 623 compounds, 58 were determined to be screening hits (as opposed to 59 of the other 4147). We calculated a nominal  $p$ -value for these results using Fisher's exact text, implemented in MATLAB release R2018b.

**Microscopy. HCFM Assay.** Live INS-1E cells were stained with the DNA dye Hoechst 33342 (all cells), Caspase 3/7 activation dye CellEvent Caspase-3/7 (apoptotic cells), and live cell impermeable DNA dye DRAQ7 (dead cells) all at 1:5000 dilution for 1.5 h. Cells were imaged at the magnification 5 $\times$  and 10 $\times$  using an Opera Phenix High-Content Imaging Instrument (PerkinElmer). Caspase-negative/positive and DRAQ7-negative/positive cells were quantified using Harmony software (PerkinElmer).

**Human Islet Staining.** Human islets were fixed with 3% PFA for 20 min, permeabilized with 0.2% Triton X-100 in PBS for 20 min, blocked with 2% BSA in PBS for 2–3 h at room temperature with gentle shaking, and then incubated with C-peptide antibody (Developmental Studies Hybridoma Bank, GN-ID4) in 2% BSA in PBS overnight at 4  $^{\circ}$ C. After thorough washing with PBS and 1% BSA in PBS, cells were incubated with secondary antibody conjugated to AlexaFluor 568 (Invitrogen) and Hoechst 33342, all in 2% BSA dissolved in PBS for 1 h at room temperature. Cells are washed five times with PBS and then stored at 4  $^{\circ}$ C. Cells were imaged at the magnification 10 $\times$  and 20 $\times$  using an

Opera Phenix high-content imaging instrument (PerkinElmer), and percent C-peptide positive cells quantified using Harmony software (PerkinElmer).

**Calcium Content.** Intracellular calcium content was quantified as previously described.<sup>14</sup> INS-1E cells plated in 384-well plates were incubated with GLT media and compound treatment for 48 h. Lyophilized Calcium 6 dye (VWR Scientific) was resuspended in GLT media and added at 1:1 volume to each well. Plates were incubated for 2 h at 37  $^{\circ}$ C where Hoechst 33342 was added at a 1:1000 ratio at 1.5 h, and imaged with 10 $\times$  and 20 $\times$  air objectives using an Operetta automated microscope (PerkinElmer). Increased calcium flux was estimated by quantifying FITC emission. Increased fluorescence in the FITC channel correlated with increased calcium content. Per cell FITC fluorescence was quantified using Hoechst to identify cell nucleus and nearby cytoplasm.

**Proinflammatory Cytokine Treatment.** Immune stress was induced as previously described.<sup>49</sup> INS-1E cells were plated at 8000 cells per well in a 384-well plate coated with an 804G matrix and incubated at 37  $^{\circ}$ C overnight. Basal media was then removed and replaced with media containing cytokines (R&D Systems) specifically RPMI media, 1% FBS, 10 ng/mL IL-1 $\beta$ , 100 ng/mL IFN- $\gamma$ , and 25 ng/mL TNF- $\alpha$ . Working concentrations of compounds were printed into the 384-well plates using a Tecan D300e drug printer. Plates were incubated at 37  $^{\circ}$ C for 48 h, and cell viability was detected using HCFM assay.

**Flow Cytometry.** Mitochondrial depolarization in INS-1E was detected using flow cytometry via the JC-1 dye. Four million treated INS-1E cells were incubated with 15.3  $\mu$ M JC-1 for 10 min, washed with dye-free RPMI 1640 medium, then trypsinized, and resuspended in dye-free RPMI 1640. Cells were sorted on a flow cytometer (Cytotrex, Beckman Coulter), and resulting data were analyzed using FlowJo flow cytometry analysis software (BD Biosciences).

**Statistical Analysis.** *In vitro* experiments were performed at least three times and quantitative data are presented as mean  $\pm$  SD. Group means were compared using ANOVA assuming Gaussian distribution followed by a one-way *t*-test. Statistical analyses were performed using GraphPad Prism software version 8 (GraphPad Software).

**Gene Expression.** Cellular RNA was isolated from INS-1E cells 24–48 h after GLT treatment using an RNeasy Plus Mini Kit (Qiagen). qPCR was performed using purified RNA, a TaqMan RNA-to-Ct 1-Step Kit (ThermoFisher), and the following TaqMan probes (ThermoFisher): Hprt1 (Rn01527840\_m1), Mrpl19 (Rn01425270\_m1), and Pdx1 (Rn00755591\_m1). qPCR samples were normalized to Hprt1 and Mrpl19 expression levels. Pdx1 expression levels were normalized relative to basal treated INS-1E.

## ■ ASSOCIATED CONTENT

### SI Supporting Information

The Supporting Information is available free of charge at <https://pubs.acs.org/doi/10.1021/acscchembio.2c00052>.

Assay development data for the GLT assay, the high-content fluorescence microscopy (HCFM) assay, and flow cytometry; compound validation data using the HCFM assay, Pdx1 expression, and effects on inflammatory cytokine-induced apoptosis; and full screening results, hit annotations, human islet donor information, and cross-assay reactivity analysis (PDF)

Screening results of glucolipotoxicity-protective small molecules from Broad Repurposing Collection, Bioactive Library, DOS Informer Set, DOS-A Library (XLSX)

## ■ AUTHOR INFORMATION

### Corresponding Author

**Bridget K. Wagner** — *Chemical Biology and Therapeutics Science Program, Broad Institute, Cambridge, Massachusetts 02142, United States*; [orcid.org/0000-0002-2629-361X](https://orcid.org/0000-0002-2629-361X); Email: [bwagner@broadinstitute.org](mailto:bwagner@broadinstitute.org)

### Authors

**Jonnell C. Small** — *Chemical Biology and Therapeutics Science Program, Broad Institute, Cambridge, Massachusetts 02142, United States; Chemistry Biology Program, Harvard Medical School, Boston, Massachusetts 02115, United States*

**Aidan Joblin-Mills** — *School of Biological Sciences and Maurice Wilkins Centre for Molecular Biodiscovery, Victoria University of Wellington, Wellington 6140, New Zealand*

**Kaycee Carbone** — *Chemical Biology and Therapeutics Science Program, Broad Institute, Cambridge, Massachusetts 02142, United States*

**Maria Kost-Alimova** — *Center for the Development of Therapeutics, Broad Institute, Cambridge, Massachusetts 02142, United States*

**Kumiko Ayukawa** — *Chemical Biology and Therapeutics Science Program, Broad Institute, Cambridge, Massachusetts 02142, United States; JT Pharmaceuticals Inc., Takatsuki 569-1125, Japan*

**Carol Khodier** — *Center for the Development of Therapeutics, Broad Institute, Cambridge, Massachusetts 02142, United States*

**Vlado Dancik** — *Chemical Biology and Therapeutics Science Program, Broad Institute, Cambridge, Massachusetts 02142, United States*

**Paul A. Clemons** — *Chemical Biology and Therapeutics Science Program, Broad Institute, Cambridge, Massachusetts 02142, United States*

**Andrew B. Munkacsi** — *School of Biological Sciences and Maurice Wilkins Centre for Molecular Biodiscovery, Victoria University of Wellington, Wellington 6140, New Zealand*; [orcid.org/0000-0003-3033-395X](https://orcid.org/0000-0003-3033-395X)

Complete contact information is available at: <https://pubs.acs.org/10.1021/acscchembio.2c00052>

### Notes

The authors declare no competing financial interest.

## ■ ACKNOWLEDGMENTS

We thank R. Elgamil, K. Emmith, N. Pirete, J. Santos, and T. Urashima for valuable advice and technical support. This work was supported by the NIH Human Islet Research Network (HIRN; U01DK123717, B.K.W.) and the Maurice Wilkins Centre for Molecular Biodiscovery (A.J.M. and A.B.M.). The authors gratefully acknowledge the use of the Opera Phenix High-Content/High-Throughput imaging system at the Broad Institute, funded by the S10 Grant NIH OD-026839-01 (B.K.W.).

## ■ REFERENCES

- (1) Boden, G. Obesity and free fatty acids. *Endocrinol Metab. Clin. N. Am.* **2008**, *37*, 635–646.
- (2) Lytrivi, M.; Castell, A. L.; Poutout, V.; Cnop, M. Recent insights into mechanisms of  $\beta$ -cell lipo- and glucolipotoxicity in type 2 diabetes. *J. Mol. Biol.* **2020**, *432*, 1514–1534.
- (3) Leung, M. B. W.; Choy, K. W.; Copp, A. J.; Pang, C. P.; Shum, A. S. W. Hyperglycaemia potentiates the teratogenicity of retinoic acid in diabetic pregnancy in mice. *Diabetologia* **2004**, *47*, 515–522.
- (4) Kashyap, S.; Belfort, R.; Gastaldelli, A.; Pratipanawatr, T.; Berria, R.; Pratipanawatr, W.; Bajaj, M.; Mandarino, L.; DeFronzo, R.; Cusi, K. A sustained increase in plasma free fatty acids impairs insulin secretion in nondiabetic subjects genetically predisposed to develop type 2 diabetes. *Diabetes* **2003**, *52*, 2461–2474.
- (5) Storgaard, H.; Jensen, C. B.; Vaag, A. A.; Vølund, A.; Madsbad, S. Insulin secretion after short- and long-term low-grade free fatty acid infusion in men with increased risk of developing type 2 diabetes. *Metabolism* **2003**, *52*, 885–894.
- (6) Prentki, M.; Corkey, B. E. Are the  $\beta$ -cell signaling molecules malonyl-CoA and cystolic long-chain acyl-CoA implicated in multiple tissue defects of obesity and NIDDM? *Diabetes* **1996**, *45*, 273–283.
- (7) Poutout, V.; Amyot, J.; Semache, M.; Zarrrouki, B.; Hagman, D.; Fontés, G. Glucolipotoxicity of the pancreatic beta cell. *Biochim. Biophys. Acta Mol. Cell Biol. Lipids* **2010**, *1801*, 289–298.
- (8) Kim, J.-W.; Yoon, K.-H. Glucolipotoxicity in pancreatic  $\beta$ -cells. *Diabetes Metab J.* **2011**, *35*, 444.
- (9) Rojas, J.; Bermudez, V.; Palmar, J.; Martínez, M. S.; Olivar, L. C.; Nava, M.; Tomey, D.; Rojas, M.; Salazar, J.; Garicano, C.; et al. Pancreatic beta cell death: novel potential mechanisms in diabetes therapy. *J. Diabetes Res.* **2018**, *2018*, 9601801.
- (10) Hagman, D. K.; Hays, L. B.; Parazzoli, S. D.; Poutout, V. Palmitate inhibits insulin gene expression by altering Pdx-1 nuclear localization and reducing MafA expression in isolated rat islets of langerhans. *J. Biol. Chem.* **2005**, *280*, 32413–32418.
- (11) Kim, J. H.; Kim, D. J.; Jang, H. C.; Choi, S. H. Epidemiology of micro- and macrovascular complications of type 2 diabetes in Korea. *Diabetes Metab J.* **2011**, *35*, 571.
- (12) Lee, S. H.; Cunha, D.; Piermarocchi, C.; Paternostro, G.; Pinkerton, A.; Ladriere, L.; Marchetti, P.; Eizirik, D. L.; Cnop, M.;

- Levine, F. High-throughput screening and bioinformatic analysis to ascertain compounds that prevent saturated fatty acid-induced  $\beta$ -cell apoptosis. *Biochem. Pharmacol.* **2017**, *138*, 140–149.
- (13) Ardestani, A.; Li, S.; Annamalai, K.; Lupse, B.; Geravandi, S.; Dobrowski, A.; Yu, S.; Zhu, S.; Baguley, T. D.; Surakattula, M.; et al. Neratinib protects pancreatic beta cells in diabetes. *Nat. Commun.* **2019**, *10*, 1–17.
- (14) Vogel, J.; Yin, J.; Su, L.; Wang, S. X.; Zessis, R.; Fowler, S.; Chiu, C. H.; Wilson, A. C.; Chen, A.; Zecri, F.; et al. A phenotypic screen identifies calcium overload as a key mechanism of  $\beta$ -cell glucolipotoxicity. *Diabetes* **2020**, *69*, 1032–1041.
- (15) Wagner, B. K.; Schreiber, S. L. The power of sophisticated phenotypic screening and modern mechanism-of-action methods. *Cell Chem. Biol.* **2016**, *23*, 3–9.
- (16) Chou, D. H. C.; Duvall, J. R.; Gerard, B.; Liu, H.; Pandya, B. A.; Suh, B. C.; Forbeck, E. M.; Faloon, P.; Wagner, B. K.; Marcaurelle, L. A. Synthesis of a novel suppressor of  $\beta$ -cell apoptosis via diversity-oriented synthesis. *ACS Med. Chem. Lett.* **2011**, *2*, 698–702.
- (17) Maianti, J. P.; Tan, G. A.; Vetere, A.; Welsh, A. J.; Wagner, B. K.; Seeliger, M. A.; Liu, D. R. Substrate-selective inhibitors that reprogram the activity of insulin-degrading enzyme. *Nat. Chem. Biol.* **2019**, *15*, 565–574.
- (18) Wang, P.; Alvarez-Perez, J. C.; Felsenfeld, D. P.; Liu, H.; Sivendran, S.; Bender, A.; Kumar, A.; Sanchez, R.; Scott, D. K.; Garcia-Ocaña, A.; et al. A high-throughput chemical screen reveals that harmine-mediated inhibition of DYRK1A increases human pancreatic beta cell replication. *Nat. Med.* **2015**, *21*, 383–388.
- (19) Ciregia, F.; Bugliani, M.; Ronci, M.; Giusti, L.; Boldrini, C.; Mazzoni, M. R.; Mossuto, S.; Grano, F.; Cnop, M.; Marselli, L.; et al. Palmitate-induced lipotoxicity alters acetylation of multiple proteins in clonal  $\beta$  cells and human pancreatic islets. *Sci. Rep.* **2017**, *7*, 13445.
- (20) Stone, V. M.; Dhayal, S.; Smith, D. M.; Lenaghan, C.; Brocklehurst, K. J.; Morgan, N. G. The cytoprotective effects of oleoylethanolamide in insulin-secreting cells do not require activation of GPR119. *Br. J. Pharmacol.* **2012**, *165*, 2758–2770.
- (21) Xiong, X.; Sun, X.; Wang, Q.; Qian, X.; Zhang, Y.; Pan, X.; Dong, X. C. SIRT6 protects against palmitate-induced pancreatic  $\beta$ -cell dysfunction and apoptosis. *J. Endocrinol.* **2016**, *231*, 159–165.
- (22) Clemons, P. A.; Bittker, J. A.; Wagner, F. F.; Hands, A.; Dančík, V.; Schreiber, S. L.; Choudhary, A.; Wagner, B. K. The use of informer sets in screening: perspectives on an efficient strategy to identify new probes. *SLAS Discovery* **2021**, *26*, 855–861.
- (23) Gerry, C. J.; Schreiber, S. L. Chemical probes and drug leads from advances in synthetic planning and methodology. *Nat. Rev. Drug Discovery* **2018**, *17*, 333–352.
- (24) Wawer, M. J.; Li, K.; Gustafsdottir, S. M.; Ljosa, V.; Bodycombe, N. E.; Marton, M. A.; Sokolnicki, K. L.; Bray, M. A.; Kemp, M. M.; Winchester, E.; et al. Toward performance-diverse small-molecule libraries for cell-based phenotypic screening using multiplexed high-dimensional profiling. *Proc. Natl. Acad. Sci. U.S.A.* **2014**, *111*, 10911–10916.
- (25) Corsello, S. M.; Bittker, J. A.; Liu, Z.; Gould, J.; McCarren, P.; Hirschman, J. E.; Johnston, S. E.; Vrcic, A.; Wong, B.; Khan, M.; et al. The drug repurposing hub: a next-generation drug library and information resource. *Nat. Med.* **2017**, *23*, 405–408.
- (26) Zhu, T.; Cao, S.; Su, P.-C.; Patel, R.; Shah, D.; Chokshi, H. B.; Szukala, R.; Johnson, M. E.; Hevener, K. E. Hit identification and optimization in virtual screening: practical recommendations based on a critical literature analysis. *J. Med. Chem.* **2013**, *56*, 6560–6572.
- (27) Wlodkovic, D.; Akagi, J.; Dobrucki, J.; Errington, R.; Smith, P. J.; Takeda, K.; Darzynkiewicz, Z. Kinetic viability assays using DRAQ7 probe. *Curr. Protoc. Cytom.* **2013**, *65*, 1–10.
- (28) Kudryavtsev, I.; Serebryakova, M.; Solovjeva, L.; Svetlova, M.; Firsanov, D. Rapid detection of apoptosis in cultured mammalian cells. *Methods Mol. Biol.* **2017**, *1644*, 105–111.
- (29) Akagi, J.; Kordon, M.; Zhao, H.; Matuszek, A.; Dobrucki, J.; Errington, R.; Smith, P. J.; Takeda, K.; Darzynkiewicz, Z.; Wlodkovic, D. Real-time cell viability assays using a new anthracycline derivative DRAQ7. *Cytometry, Part A* **2013**, *83*, 227–234.
- (30) Wong, D. W.; Gan, W. L.; Teo, Y. K.; Lew, W. S. Interplay of cell death signaling pathways mediated by alternating magnetic field gradient. *Cell Death Discovery* **2018**, *4*, 49.
- (31) Hasegawa, T.; Shimada, S.; Ishida, H.; Nakashima, M. Chafuroside B, an oolong tea polyphenol, ameliorates UVB-induced DNA damage and generation of photo-immunosuppression related mediators in human keratinocytes. *PLoS One* **2013**, *8*, No. e77308.
- (32) Lowe, J. T.; Lee, M. D.; Akella, L. B.; Davoine, E.; Donckele, E. J.; Durak, L.; Duvall, J. R.; Gerard, B.; Holson, E. B.; Joliton, A.; et al. Synthesis and profiling of a diverse collection of azetidione-based scaffolds for the development of CNS-focused lead-like libraries. *J. Org. Chem.* **2012**, *77*, 7187–7211.
- (33) Maji, B.; Gangopadhyay, S. A.; Lee, M.; Shi, M.; Wu, P.; Heler, R.; Mok, B.; Lim, D.; Siriwardena, S. U.; Paul, B.; et al. A high-throughput platform to identify small-molecule inhibitors of CRISPR-Cas9. *Cell* **2019**, *177*, 1067–1079 E19.
- (34) Dančík, V.; Carrel, H.; Bodycombe, N. E.; Petri Seiler, K.; Fomina-Yadlin, D.; Kubicek, S. T.; Hartwell, K.; Shamji, A. F.; Wagner, B. K.; Clemons, P. A. Connecting small molecules with similar assay performance profiles leads to new biological hypotheses. *J. Biomol. Screen* **2014**, *19*, 771–781.
- (35) Harwood, H. J.; Petras, S. F.; Shelly, L. D.; Zaccaro, L. M.; Perry, D. A.; Makowski, M. R.; Hargrove, D. M.; Martin, K. A.; Tracey, W. R.; Chapman, J. G.; et al. Isozyme-nonspecific N-substituted bipiperidylcarboxamide acetyl-CoA carboxylase inhibitors reduce tissue malonyl-CoA concentrations, inhibit fatty acid synthesis, and increase fatty acid oxidation in cultured cells and in experimental animals. *J. Biol. Chem.* **2003**, *278*, 37099–37111.
- (36) Kornelius, E.; Li, H.-H.; Peng, C.-H.; Yang, Y.-S.; Chen, W.-J.; Chang, Y.-Z.; Bai, Y.-C.; Liu, S.; Huang, C.-N.; Lin, C.-L. Liraglutide protects against glucolipotoxicity-induced RIN-m5F  $\beta$ -cell apoptosis through restoration of PDX1 expression. *J. Cell Mol. Med.* **2019**, *23*, 619–629.
- (37) Law, B. Y. K.; Mok, S. W. F.; Chen, J.; Michelangeli, F.; Jiang, Z.-H.; Han, Y.; Qu, Y. Q.; Qiu, A. C. L.; Xu, S.-W.; Xue, W.-W.; et al. N-desmethylauricidine induces autophagic cell death in apoptosis-defective cells via Ca<sup>2+</sup> mobilization. *Front. Pharmacol.* **2017**, *8*, 388.
- (38) Perelman, A.; Wachtel, C.; Cohen, M.; Haupt, S.; Shapiro, H.; Tzur, A. JC-1: alternative excitation wavelengths facilitate mitochondrial membrane potential cytometry. *Cell Death Dis.* **2012**, *3*, No. e430.
- (39) Chou, D. H.-C.; Vetere, A.; Choudhary, A.; Scully, S. S.; Schenone, M.; Tang, A.; Gomez, R.; Burns, S. M.; Lundh, M.; Vital, T.; et al. Kinase-independent small-molecule inhibition of JAK-STAT signaling. *J. Am. Chem. Soc.* **2015**, *137*, 7929–7934.
- (40) Trivedi, P. M.; Graham, K. L.; Scott, N. A.; Jenkins, M. R.; Majaw, S.; Sutherland, R. M.; Fynch, S.; Lew, A. M.; Burns, C. J.; Krishnamurthy, B.; et al. Repurposed JAK1/JAK2 inhibitor reverses established autoimmune insulinitis in NOD mice. *Diabetes* **2017**, *66*, 1650–1660.
- (41) Liu, M.; Wright, J.; Guo, H.; Xiong, Y.; Arvan, P. Proinsulin entry and transit through the endoplasmic reticulum in pancreatic beta cells. *Vitam Horm.* **2014**, *95*, 35–62.
- (42) Leighton, E.; Sainsbury, C. A.; Jones, G. C. A ractical review of C-peptide testing in diabetes. *Diabetes Ther.* **2017**, *8*, 475–487.
- (43) Joly, E.; Prentki, M.; Buteau, J.; El-Assaad, W.; Rhodes, C. J.; Rosenberg, L. Glucagon-like peptide-1 prevents beta cell glucolipotoxicity. *Diabetologia* **2004**, *47*, 806–815.
- (44) Shao, S.; Nie, M.; Chen, C.; Chen, X.; Zhang, M.; Yuan, G.; Yu, X.; Yang, Y. Protective action of liraglutide in beta cells under lipotoxic stress via PI3K/Akt/FoxO1 pathway. *J. Cell. Biochem.* **2014**, *115*, 1166–1175.
- (45) Mao, G.-H.; Lu, P.; Wang, Y.-N.; Tian, C.-G.; Huang, X.-H.; Feng, Z.-G.; Zhang, J.-L.; Chang, H.-Y. Role of PI3K p110 $\beta$  in the differentiation of human embryonic stem cells into islet-like cells. *Biochem. Biophys. Res. Commun.* **2017**, *488*, 109–115.
- (46) Parnaud, G.; Hammar, E.; Ribaux, P.; Donath, M. Y.; Berney, T.; Halban, P. A. Signaling pathways implicated in the stimulation of  $\beta$ -Cell proliferation by extracellular matrix. *Mol. Endocrinol.* **2009**, *23*, 1264–1271.

- (47) Walpita, D.; Wagner, B. K. Evaluation of compounds in primary human islet cell culture. *Curr. Protoc. Chem. Biol.* **2014**, *6*, 157–168.
- (48) Zhang, J. H.; Chung, T. D.; Oldenburg, K. R. A simple statistical parameter for use in evaluation and validation of high throughput screening assays. *J. Biomol. Screen* **1999**, *4*, 67–73.
- (49) Chou, D. H. C.; Holson, E. B.; Wagner, F. F.; Tang, A. J.; Maglathlin, R. L.; Lewis, T. A.; Schreiber, S. L.; Wagner, B. K. Inhibition of histone deacetylase 3 protects beta cells from cytokine-induced apoptosis. *Chem. Biol.* **2012**, *19*, 669–673.